

Cytoskeletal Deformation at High Strains and the Role of Cross-link Unfolding or Unbinding

HYUNGSUK LEE,¹ BENJAMIN PELZ,³ JORGE M. FERRER,² TAEYOON KIM,¹ MATTHEW J. LANG,^{1,2}
and ROGER D. KAMM^{1,2}

¹Department of Mechanical Engineering, Massachusetts Institute of Technology, Cambridge, MA 02139, USA; ²Department of Biological Engineering, Massachusetts Institute of Technology, Cambridge, MA 02139, USA; and ³Physik-Department E22, Technische Universität München, D-85748 Garching b. Munich, Germany

(Received 19 January 2009; accepted 2 February 2009; published online 12 February 2009)

Abstract—Actin cytoskeleton has long been a focus of attention due to its biological significance and unique rheological properties. Although F-actin networks have been extensively studied experimentally and several theoretical models proposed, the detailed molecular interactions between actin binding proteins (ABPs) and actin filaments that regulate network behavior remain unclear. Here, using an *in vitro* assay that allows direct measurements on the bond between one actin cross-linking protein and two actin filaments, we demonstrate force-induced unbinding and unfolding of filamin. The critical forces prove to be similar, 70 ± 23 pN for unbinding and 57 ± 19 pN for unfolding, suggesting that both are important mechanisms governing cytoskeletal rheology. We also obtain the mechanical response of a cross-linked F-actin network to an optically trapped microbead and observe abrupt transitions implying rupture or unfolding of cross-links. These measurements are interpreted with the aid of a computational simulation of the experiment to provide greater insight into physical mechanisms.

Keywords—F-actin, Filamin, Single molecule, Network.

INTRODUCTION

Cytoskeletal rheology has captured the interest of many researchers because of its importance in telegraphing numerous biological processes, but also due to the rich variety of observed behavior. At small amplitude, the complex shear modulus *in vivo* typically exhibits a weak power law, undergoing a transition from primarily elastic behavior at low frequencies to one dominated by viscous effects at high frequency.^{5,8} Attempts to reproduce these characteristics in the linear regime using *in vitro* systems,^{32,39,40} typically a reconstituted actin gel with one or more cross-linking

proteins present, have met with limited success. Early experiments found a much higher frequency dependence with values of shear modulus that were orders of magnitude lower than those observed in cells. More recently, it has been shown that network prestrain plays a critical role, stiffening the matrix to the point that moduli become comparable to the *in vivo* values.^{11,12} Even then, however, the modulus exhibits a different frequency dependence, ranging from nearly constant value for the storage modulus (G') at low frequencies, with a gradual transition to a weak power law at higher frequencies. To complicate the situation further, different cross-linking proteins apparently affect the linear rheological behavior in different ways, depending in part on whether the network forms large-diameter bundles (stress fibers),²³ or organizes the actin filaments into a more orthogonal network.³⁴ Many of these fascinating characteristics remain unexplained, but have been a source of much recent debate.

A similar range of views also exist in the modeling community. Various models have been proposed and each has its own proponents. These can be classified into several broad categories, which can be characterized as the cellular solids model, the tensegrity model, and the biopolymer model. In the tensegrity model,²⁰ an interaction is proposed between certain elements that are in tension and others that are under a compressive state. These latter could either be internal structures such as the microtubules or external tethering to a substrate or extracellular matrix. Theoretical descriptions of tensegrity show that the storage modulus depends primarily upon the level of prestrain in the network and is relatively independent of the properties of the matrix elements themselves. In contrast, the cellular solids model is based on earlier description of macroscopic fibrous materials,^{13,14} in which the elastic behavior is entirely determined by the bending stiffness of the elastic fibers and the fiber concentration. Neither of these models have been

Address correspondence to Roger D. Kamm, Department of Mechanical Engineering, Massachusetts Institute of Technology, Cambridge, MA 02139, USA. Electronic mail: rdkamm@mit.edu

extended to include viscoelastic behavior, so they provide no information on the unique frequency dependence described above. One can also view the actin network as a semi-dilute solution of polymers, the biopolymer model, with or without cross-links that are thermally active. Because of the long persistence length of actin, the individual filaments of an actin gel exhibit slight deviations from straight segments between cross-link points, but these slight fluctuations provide for the network elasticity at low strains. Recent models have incorporated the effects of prestrain, and produce predictions that capture some of the nonlinear behavior.³³

Based on these previous experimental studies and models, despite many fundamental differences, the prevailing view is that prestrain is a critical factor. In living cells, this can result from a combination of external tethering via an assortment of adhesion receptors and internal contraction due to the activity of myosin motors and other forces that associate with the actin filaments. In this highly prestrained condition, the cross-links are subjected to relatively high loads, likely sufficient to cause them to either unfold or unbind, giving rise to entirely new phenomena such as matrix irreversibility and network remodeling under stress. While unfolding and unbinding can both give rise to a certain degree of hysteresis, the underlying mechanisms and relevant time scales will differ. For example, if a strained cross-link unbinds, the filaments will locally rearrange, and the “dangling” cross-linking protein might form a new bond at a different location in the network, potentially (but not necessarily) resulting in a new equilibrium state of a remodeled network. If this same cross-linker unfolds, when the stress is released, the protein may refold given sufficient time, and return to the original state. Both the time scales for reaching equilibrium and the potential for remodeling differ in these two scenarios, and it therefore becomes an important question as to whether unbinding or unfolding is the dominant behavior in high stress states, especially given the perceived importance of high prestrain or prestress in living cells.

Here we explore the question of whether unfolding or unbinding is more likely to occur. In order to address this question, we examine recent experiments from our own laboratory and those from others, as well as new data that extend our previous work. We rely primarily upon two methods employing an optical trap that provide insight into single molecule events. One is a single molecule pulling assay in which a single actin filament forms a tether with another actin filament via one specific cross-linker, and an optical trap is used to precisely control the applied force. Another method is introduced, in which the mechanical response of a reconstituted actin gel to a local force is

monitored, providing insights into single molecule events in a 3-dimensional network. In the isolated single molecule measurement, unfolding is distinguished from unbinding by the sawtooth pattern with intervals ~ 30 nm observed in the force-extension curves. Both unfolding and unbinding occur at similar levels of force, but unbinding is more frequent than unfolding. Further analysis of measurements at different pulling angles suggests that torsion or shear induce rupture at smaller force. Compared with the results from single molecule assays, the responses of an F-actin network also show similar transitions in the force-extension curves indicating that similar events, both bond rupture and unfolding, can be identified, holding open the promise of analyzing single molecule events within a 3-dimensional network.

MATERIALS AND METHODS

Protein Preparation

G-actin is prepared by dissolving lyophilized G-actin from rabbit skeletal muscle (Cytoskeleton Inc., Denver, CO) in fresh G-buffer [5 mM Tris-HCl, 0.2 mM CaCl₂, 0.5 mM DTT, 0.2 mM ATP, pH 8.0] and incubated on ice for ~ 2 h. For biotinylated actin filaments, 20 μ L of 20 μ M nonlabeled actin monomer is mixed with 5 μ L of 20 μ M biotinylated actin (Cytoskeleton Inc., Denver, CO). Actin polymerization is initiated by adding a tenth of the final volume of 10 \times F-buffer [50 mM Tris-HCl, 500 mM KCl, 2 mM MgCl₂, 2 mM CaCl₂, 2 mM DTT, 5 mM ATP, 0.01% (w/v) NaN₃, pH 7.5]. Recombinant filamin A is purified from Sf9 cell lysates²⁹ and recombinant human gelsolin is produced in *Escherichia coli*.²⁴ Both were stored at -80 °C before use.

Microsphere Attachment to an Actin Filament

One micrometer diameter, carboxylated polystyrene beads (Polysciences Inc., Warrington, PA) are coated with gelsolin as described in Suzuki *et al.*³⁵ with the 400 μ g proteins: 5 μ L of 10 mg/mL actin, 10 μ L of 5 mg/mL gelsolin, 26 μ L of 10 mg/mL bovine serum albumin (BSA), and 40 μ L of 1 mg/mL rhodamine-BSA. The gelsolin-coated beads are stored in a rotator at 4 °C in the dark. Twenty-five microliters of bead solution is diluted with 25 μ L of the buffer solution [25 mM imidazole-HCl (pH 7.4), 25 mM KCl, 4 mM MgCl₂, 0.1 mM CaCl₂, 0.1 mM ATP, 1 mM DTT, and 0.04% NaN₃] and sonicated for 30 s. The bead solution is washed four times with 50 μ L of the same buffer by centrifugation at 6000 rpm for 4 min. After the last centrifugation, the beads are resuspended with 10 μ L buffer solution and are mixed with 2.5 μ L of

5 μM F-actin labeled with rhodamine-phalloidin. The mixture is incubated overnight in a rotator at 4 $^{\circ}\text{C}$ in the dark. Under these concentrations of bead and F-actin, a microsphere bound to a single actin filament is obtained.

Single Molecule Pulling Assay

A custom-made flow chamber (25.8 mm \times 6 mm \times 0.1 mm) is prepared by attaching a KOH-etched coverslip to a microscope slide with double-sided tape. The sample is loaded from one end and the flow of sample solution is facilitated by using a pipette tip connected to a vacuum pump. The experimental sample is prepared by the following procedure: (1) incubation of 2 mg/mL biotinylated BSA in PBT [100 mM phosphate buffer (pH 7.5), 0.1% (v/v) Tween, pH 7.5]; (2) washing with PBT; (3) incubation of 0.1 mg/mL streptavidin in PBT; (4) washing with 1 \times F-buffer containing with 3 mg/mL BSA; (5) incubation of 50 mM biotinylated actin filament in 1 \times F-buffer containing 3 mg/mL BSA; (6) washing with 1 \times F-buffer containing 3 mg/mL BSA; (7) incubation of 20 nM filamin in 1 \times F-buffer with 3 mg/mL BSA; (8) incubation of F-actin bound to gelsolin bead in a 1:100 dilution. Twenty microliters of sample solution is loaded in each incubation step and 100 μL of buffer is used in washing. Incubation steps are performed for 20 min in a dark, humidity-preserving chamber at room temperature. The flow chamber is sealed with nail polish to prevent evaporation of the sample during the experiment.

Beads tethered to the actin filament are readily distinguished from other beads by a confined movement. Approximately 20–30 tethered beads are observed per field of view. Optical tweezers force spectroscopy (OTFS) is used to probe interaction between the actin filament and filamin (Fig. 1). Tethered beads are located and centered in the detection zone using an automated centering routine and are captured by the stationary trapping laser with the stiffness ranging from 0.5 to 0.75 pN/nm. Force is applied to a complex comprised of one filamin protein cross-linking two actin filaments by translating the sample relative to the trap at a constant speed of 5 $\mu\text{m/s}$. At the same time, the displacement of the bead is monitored with the detection laser. Actual bead position and trap stiffness are calibrated after each measurement as described previously.²⁵

Assay for Cross-Linked F-Actin Networks

Solutions of gelsolin, filamin, microspheres, and 10 \times F-buffer are gently mixed to induce polymerization. After addition of G-actin, the final solution is loaded into the custom-made flow chamber within

10 s. The sample is polymerized for 2 h at room temperature and the chamber is sealed with nail polish. Final concentration of actin is 10 μM , and the molar ratio of filamin to actin is 0.01. The gelsolin concentration used in these experiments regulates the average length of actin filament to be approximately 5 μm .

Optical tweezers are used to apply a local force to a cross-linked F-actin network and observe the response. In a similar manner to the method described above, an embedded bead is captured and the stage is translated in one direction to apply a local force to the network. The stage speed is a constant 5 $\mu\text{m/s}$. The force applied to the network can be estimated by multiplying the distance of the microsphere from the center of the trap by the stiffness of the trap.

Experimental Setup Using the OTFS

Experiments are performed using a highly automated custom-built optical trap described previously.⁴ The 1064 nm trapping laser (Coherent, Santa Clara, CA) is focused by a high numerical aperture objective (100 \times , 1.40 NA, oil IR; Nikon, Tokyo, Japan) on the specimen plane to capture a 1 μm diameter microsphere. A pair of acousto-optic deflectors (AODs; Intra-Action, Bellwood, IL) enables rapid control of the location of the trap in two dimensions while the position of the trapped bead is monitored by a 975 nm laser beam imaged on a position sensitive device (PSD, Pacific Silicon, West Lake Village, CA) for back-focal plane position detection.¹⁵ The output voltage from the PSD is collected by a 16-bit A/D board (National Instruments, Austin, TX), and is saved as a txt file by a custom software (LabView; National Instruments, Austin, TX). Bead positions are recorded at 3–10 kHz, which is fast enough to resolve the position of the bead displacement with increments of <1 nm extension at our loading rate. After rupture in each experimental run, the bead position and trap stiffness are determined using previously described procedures.^{25,31}

Computational Model

A 3-dimensional actin network is generated via the polymerization and cross-linking of an initial structure with uniformly distributed actin monomers and randomly dispersed actin cross-linking proteins which form an orthogonal network like filamin using methods previously described.²² Actin concentration of the network used in this study is 12 μM , the average length of the actin filaments is \sim 1.5 μm , and the molar ratio of ABP to actin is 0.017. The width of a cubical computation domain is 5 μm . Motions of actin filaments and ABPs are governed by Brownian dynamics, and they

are also characterized by appropriate bending and extensional stiffness. After polymerization, all actin filaments are severed and clamped at the upper and lower boundaries (z -surfaces), and periodic boundary conditions are imposed on all other boundaries (x - and y -surfaces). A microbead with the diameter of $1.2\ \mu\text{m}$ is then inserted into the actin network by replacing all filaments within a central spherical region with a rigid sphere. To simulate the network experiments, the microbead is forced to move in $+x$ direction with the constant rate of $20\ \mu\text{m/s}$. During the simulation, unbinding of ABP follows Bell's equation with $k_{\text{off}} = 0.115\ \text{s}^{-1}$ and $x^{\ddagger} = 0.416\ \text{nm}$; only extensional forces acting on the ABPs are considered. Both the sum of forces acting on the microbead in x direction and the state of each ABP (bound or free) are recorded as functions of bead displacement.

RESULTS

Force-Induced Unbinding of Filamin

In single molecule experiment, a typical force-extension curve (Fig. 2a) exhibits an initial gradual increase in force that rapidly accelerates as extension increases. When the force reaches a critical level, between 50 and 170 pN, it relaxes abruptly to a value near zero. At the loading rates of 400–2000 pN/s, multiple force peaks, ranging from two to six per pull, were generally observed indicating either reattachment of the unbound filament or multiple binding locations along a single filament. Note that the bead snaps back to its baseline location after each final break as well as for intermediate drops in traces containing multiple drops. The overall extension before rupture ranges from 500 to 2500 nm, considerably in excess of the

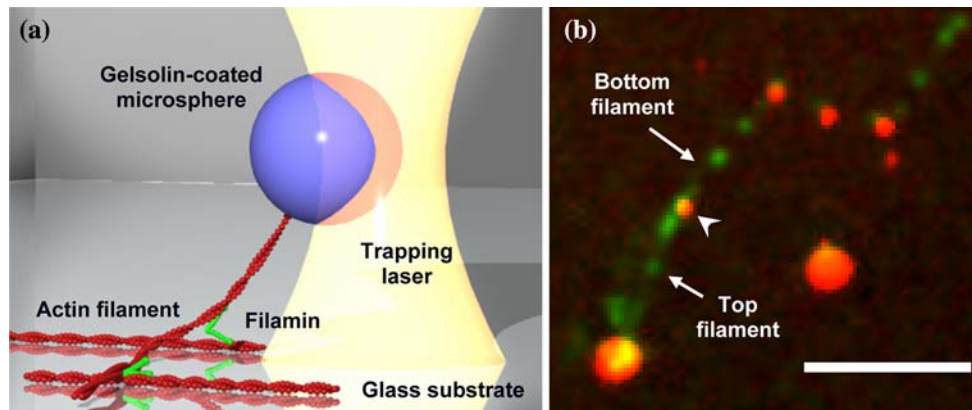


FIGURE 1. Single molecule assay. (a) The bottom actin filament is biotinylated and immobilized by bonding to a streptavidin-coated glass substrate. The top actin filament is tethered to a gelsolin coated microbead. Two actin filaments are cross-linked with ABP filamin and the stage is translated while the microsphere is constrained by the optical trap. Displacement of the microsphere is monitored to determine the force of interaction between the ABP and the actin filaments. (b) Confocal micrograph showing a complex formed by an ABP filamin (small red spots) cross-linking two actin filaments (shown in green). Actin filament and filamin were conjugated with Alexa Fluor 488 and ds-Red, respectively. The gelsolin beads (large red circles) were labeled with BSA conjugated with Alexa Fluor 555. Arrowhead indicates the cross-linking point where the top and bottom actin filaments are cross-linked (scale bar: $5\ \mu\text{m}$).

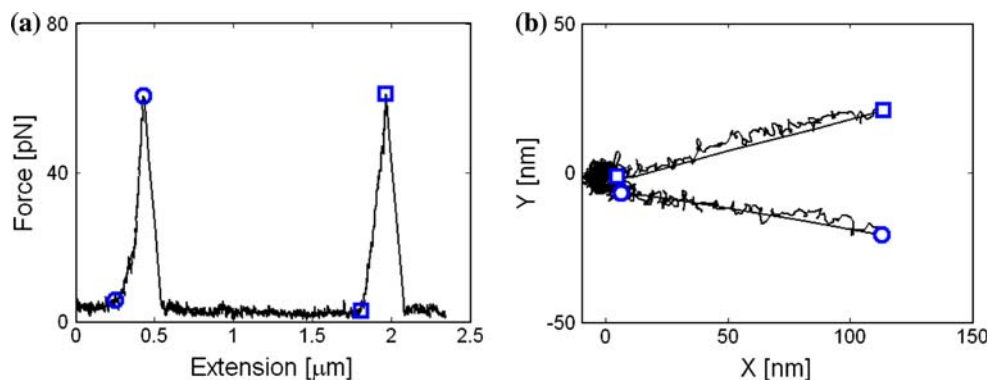


FIGURE 2. Molecular response of actin-ABP upon unbinding. (a) Force vs. extension curve showing the force increasing until the first bond rupture, then increasing again as another bond is stressed. The forces relax back to baseline, zero force, after each rupture. (b) Corresponding x - y plot showing the displacement of the bead relative to the trap center. The two different slopes indicate that two different attachment sites are probed on each pull.

contour length of filamin even when accounting for unfolding. Our assay consists of several linking components, thus this large extension is ascribed to additional compliance such as bending of actin filaments at the surface attachment point, rotation of the molecular linkages, and bending of actin filament at the bead attachment location. Also, the length of the bound actin filament and the distance between bead and cross-linking point will significantly influence the overall extension before rupture.

For each pulling measurement, we estimate the pulling rotational angle of the trapped bead by monitoring its x - and y -axis displacements. Due to the arrangement of stage and PSD with angle in our microscope, the stage movement for loading is along the x -axis in Fig. 2b. The surface bound actin filaments are generally aligned parallel to the pulling direction by washing steps shortly after flowing actin filaments. As a result, deviation from the x -axis indicates that the vector connecting the position of the trapped bead and the cross-linking point is not oriented along the pulling axis, causing the bead displacement relative to the trap

center to deviate from the x -axis, and leading to a situation in which a torque may be applied to the bond in addition to the pulling force. While this arrangement complicates the nature of the applied force, it also provides the advantage of helping to distinguish unbinding of filamin from unfolding when multiple transitions occur in a pull. Approximately 86% of rupture-like traces in which the force goes back to baseline after transition exhibit a different angle upon continued pulling confirming that a different bond is being stressed after rupture of the previous one.

Force-Induced Unfolding of Filamin

Approximately 20% of our measurements probe unfolding of Ig domains in filamin exhibiting different force-extension traces from those of unbinding events. At a critical force ranging from 29 to 94 pN, the typical trace exhibits multiple drops of 4–10 pN (6–15 nm in bead displacement) with decrease of force slope (Fig. 3a). The number of drops in the unfolding region ranges from 8 to 17. Compared to the unbinding trace

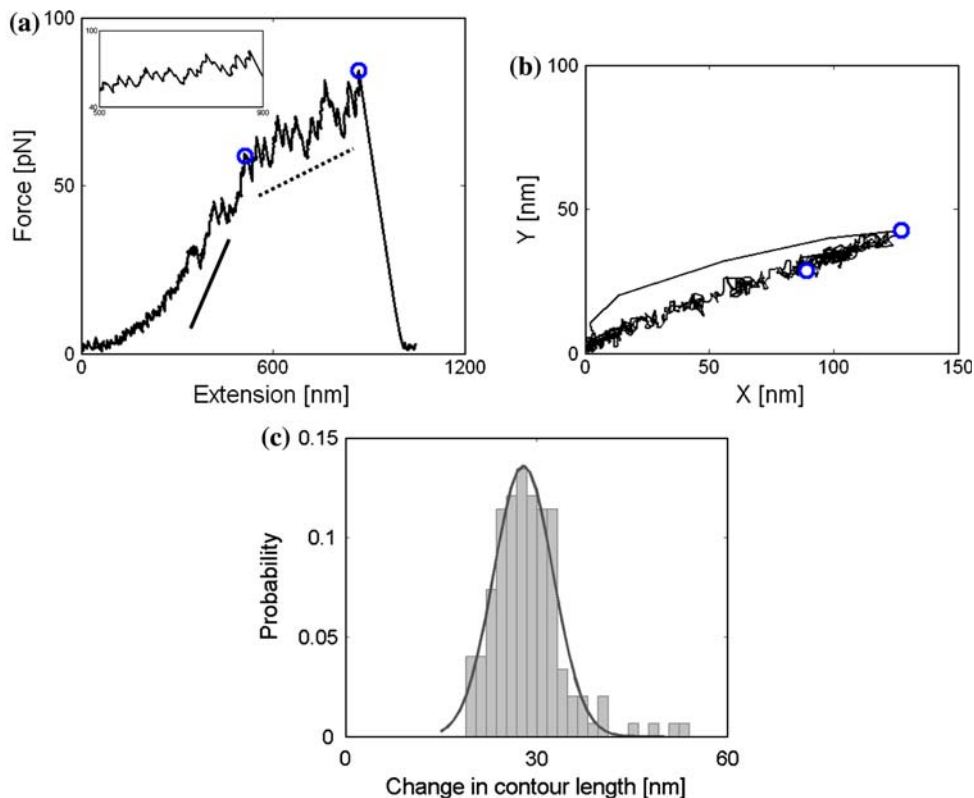


FIGURE 3. Molecular response of actin-ABP upon unfolding. (a) When the force reaches a critical value, a sawtooth like pattern is sometimes observed in the trace indicating unfolding of individual filamin Ig domains. The circle symbols indicate the start and end of the potential unfolding events. (Inset) The change in contour length by unfolding can be estimated by measuring the distance between peaks (x -axis in nm) of the trace in the enlargement of the dotted region. (b) Repeating transitions exhibited in the unfolding trace are along the same pulling trajectory. (c) Histogram of the change in contour length obtained by measuring the peak-to-peak distances from the data of the type shown in (a) ($n = 154$). Gaussian fit identifies the average value to be 28 ± 5 nm.

in Fig. 2, the force does not relax back to baseline (Fig. 3a) and the transitions follow along the same x - y trajectory (Fig. 3b), even during multiple force drops. To further characterize the period of the peaks observed in the unfolding trace, we calculate the distance between force peaks in the force-extension curves and, using a Gaussian fit, find the period between the transitions to be 28 ± 5 nm (Fig. 3c).

Force Distributions and Kinetic Parameters

We obtain the force distributions for both unbinding and unfolding by measuring the peak forces in the force-extension curves. As indicated by the overlap of two histograms in Fig. 4, force level distributions for unbinding and unfolding are remarkably similar. The force at which the unfolding and unbinding occurs is 57 ± 19 and 70 ± 23 pN, respectively. This similarity in critical force level is consistent with our observations that both unbinding and unfolding occur at the same pulling speed although unfolding is less frequent.

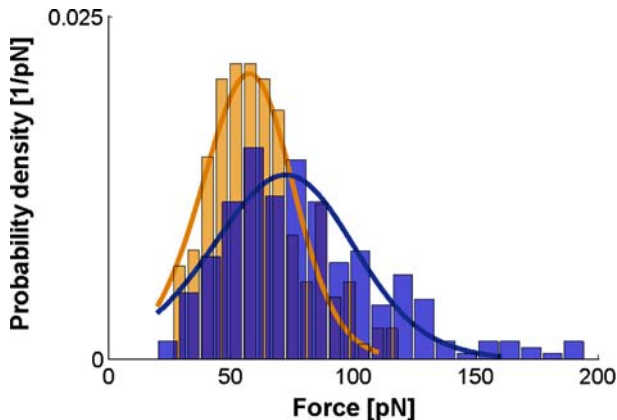


FIGURE 4. Unbinding and unfolding force distributions. Probability density functions for unbinding (blue) and unfolding (orange) are obtained by measuring the critical force at which the respective events occur. Average forces for unfolding and unbinding are 57 ± 19 and 70 ± 23 pN, respectively. HS model (solid line) provides a good fit for both force distributions and estimates the kinetic parameters, results of which are summarized in Table 1.

TABLE 1. HS model parameters.

	k_{off} (s^{-1})	x^\ddagger (nm)	κ_m (pN/nm)	ΔG (k_BT)
Loading rate (400–2000 pN/s)				
Unbinding	1.70	0.27	646	5.6
Unfolding	0.52	0.46	266	6.8
Loading rate (5–50 pN/s)				
Unbinding	0.087	0.19	820	3.6

The results for the loading rate of 5–50 pN/s⁹ were listed for comparison.

To estimate the kinetic parameters in the actin/filamin molecular interaction, we implement the theoretical model developed by Hummer and Szabo¹⁹ referred to here as the HS model. Three parameters can thus be computed from the experimental results of rupture force and loading rate; the intrinsic rate constant (k_{off}) in the absence of external force, the position of the transition state (x^\ddagger), and the molecular spring constant (κ_m) (Table 1).

Unbinding and unfolding force distributions can be fit to the model (Fig. 4), both yielding $R^2 = 0.88$. Assuming a single subunit rupture, values for apparent k_{off} are computed to be 1.70 s^{-1} for unbinding and 0.52 s^{-1} for unfolding. In the bulk scale experiment using the stopped flow method,¹⁶ k_{off} for filamin/actin binding was determined to be 0.6 s^{-1} , 2–3 times lower than our estimation. This difference may be due to the difference in measurement techniques and the dependence of unbinding force on the experimental parameters such as loading angle and speed. The transition distances for unbinding and unfolding are 0.27 nm and 0.14 nm, and the spring constants are 646 and 266 pN/nm, respectively. Given κ_m and x^\ddagger , the height of the free energy barrier, ΔG^\ddagger , can be computed as $1/2\kappa_m x^{\ddagger 2}$. For unfolding ΔG^\ddagger is 6.8 k_BT , higher than the value of 5.6 k_BT for unbinding, indicating that more energy is required for unfolding. This helps to explain why unfolding occurs less frequently than unbinding in our measurements even though the critical force levels are similar.

Angle Dependency

From the x - y plots of bead displacement, we calculate the angle for all pulling trajectories (Figs. 2b and 3b) and can therefore identify how the rupture force varies as a function of angle. No noticeable change in rupture force is observed for angles smaller than 45° (Fig. 5a). However, when the bead trajectory deviates from the pulling direction by more than 45° , rupture force decreases significantly. Similar angle dependency of rupture force is observed at both high and low loading rates. Considering a possible configuration of the proteins in our assay, filamin would be subjected to the more shear/torsional forces in addition to the extensional force as the angle increases. Therefore, this result suggests that filamin/F-actin binding ruptures at lower levels of force when shear/torsional force is applied.

Loading rate Dependency of Unbinding

We also investigated the effect of loading rate on force-induced unbinding. The loading rate is defined as the slope of a linear fit to the force vs. time trace just

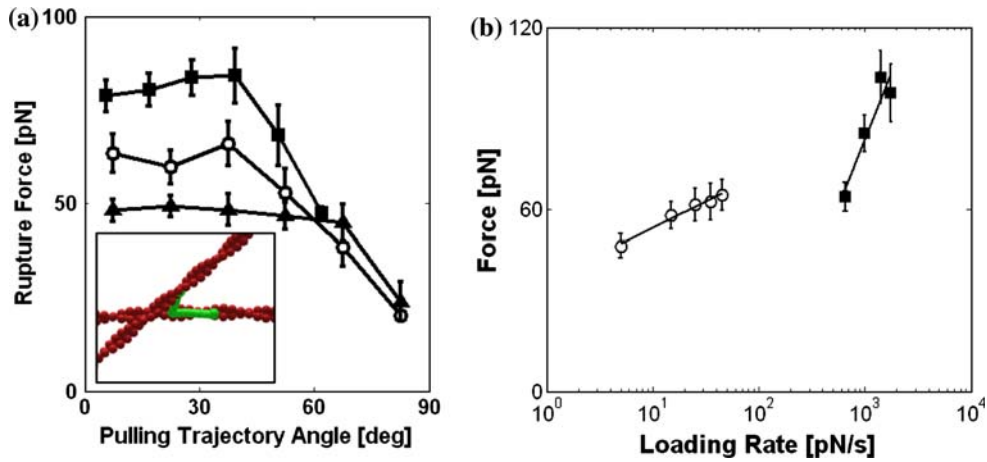


FIGURE 5. (a) Dependence of rupture on pulling angle. The pulling trajectory angle is the angle formed between the pulling direction and the direction of force acting on the bead (see text). Rupture force for filamin starts to decrease at an angle of $\sim 45^\circ$ at both low (5–50 pN/s, \circ) and high (400–2000 pN/s, \blacksquare) loading rates, while the rupture force for α -actinin⁹ exhibits a constant value up to $\sim 70^\circ$ (\blacktriangle). (Inset) Top view of the assay where two actin filaments (red) cross-linked with ABP (green) form an angle of 45° . (b) Dependence of rupture force on loading rate. The general tendency is for rupture force to increase with loading rate. However, the slope of force at the high loading rate (\blacksquare) is much higher than that at the low loading rate (\circ) in the single molecule measurements (some results adapted from Ferrer *et al.*⁹).

prior to rupture. Rupture force is observed to increase with loading rate in both low and high speed pulling regimes (Fig. 5b). A linear increase in force with the logarithm of loading rate was also observed in other molecular interactions³⁰ and agrees with theoretical predictions.^{1,7,19} The rupture force data exhibit two regimes with different slopes, implying either the presence of two barriers in the energy landscape of the filamin/F-actin binding or the occurrence of rebinding at the low loading rate. The change in the slope of force is attributed to the suppression of an outer energy barrier by external force.⁷ A similar behavior has been shown in other molecular complexes such as actomyosin, avidin–biotin, and selectin–ligand bonds.^{18,27,36,41} Previous measurements for α -actinin/F-actin rupture also found two lifetime regimes.²⁸ Since filamin and α -actinin have calponin homology actin binding domain which is a conserved sequence in other ABPs,^{6,17,26} the presence of multiple energy barriers might be a general characteristic of ABP/F-actin binding.

Response of F-Actin Network to Local Excitation

Local force is applied to the cross-linked F-actin network as the stage is displaced with the embedded microsphere captured by optical tweezers. Typical force vs. bead displacement curves exhibit multiple transitions where the force does not drop to zero (Fig. 6a), suggestive of abrupt alterations in the network surrounding the microsphere. The force at these transitions ranges from 20 to 56 pN. Further deformation of the network causes the microsphere to move

out of detection region, leading to a discontinuity in the curve. Compared with the single molecule measurements, similar transitions observed in the network's responses suggest that these originate from unbinding and unfolding of the stressed cross-linkers by deformation of actin filaments (Fig. 6b).

Computational Analysis of Network Deformation

To substantiate the importance of unbinding of individual ABPs in the mechanical response of actin networks, we also employ our computational model. As can be seen in Fig. 7, the response measured in the simulation is qualitatively similar to those in Fig. 6a: an increase in the force and the existence of multiple transitions when the force drops abruptly. During bead displacement, a number of ABP unbinding events occur (red circles on the curve), but most appear to be insignificant in that they are not reflected by any noticeable change in the force curve, except for two cases. In order to isolate the critical unbinding events, we apply two criteria: (1) the distance between the ABP and the surface of the microbead at the moment of unbinding must be < 500 nm, and (2) the ABP must lie within a cone centered on the $+x$ -axis with an included angle of $2\pi/3$. Only three rupture events meet these criteria (blue circles). Two of these correspond to the sudden transitions of the mechanical response though one occurs early in the simulations and seems irrelevant. This implies that the multiple transitions observed in the experiment can be attributable to the unbinding of ABPs in close proximity to the microbead.

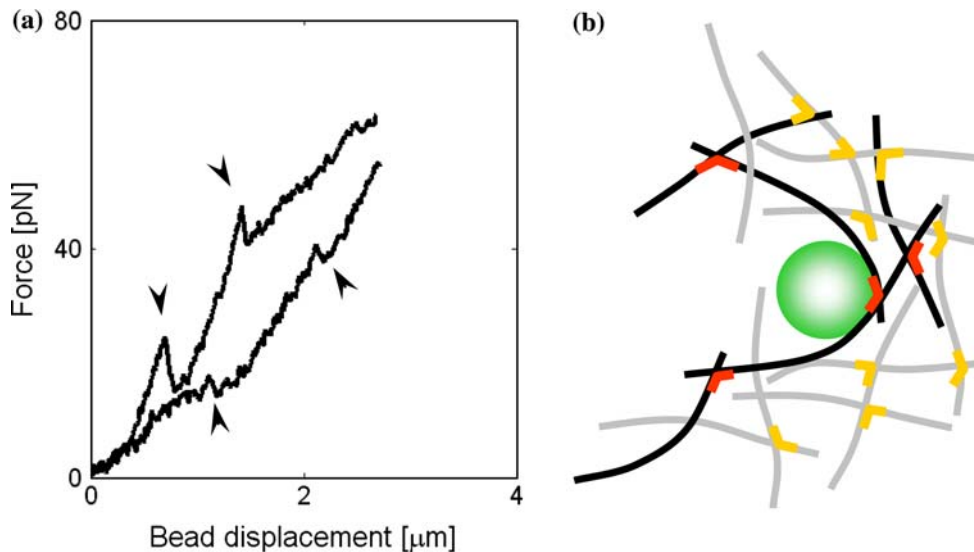


FIGURE 6. (a) Mechanical response of F-actin network to the local forcing associated with bead displacement by an optical trap. The force trace exhibits multiple transitions (arrow heads) where the force drops, but not to zero. (b) Schematic view of the bead embedded in a cross-linked F-actin network. Bead displacement deforms both F-actin (gray) and ABP (yellow) in the network. The most stressed actin filaments (black) may cause a rupture of the deformed ABPs (red) leading to an abrupt transition in bead response.

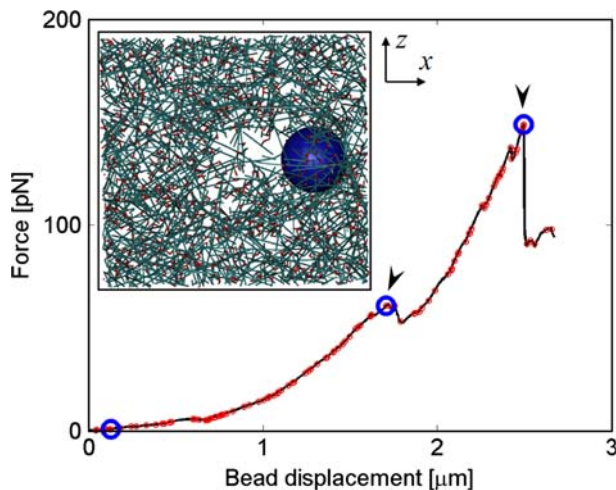


FIGURE 7. Mechanical response of an actin network simulated by a computational model. Red circles show all ABP rupture events, and blue circles show only those satisfying the two criteria described in the text. As in Fig. 6a, the force acting on the microbead rises with increased bead displacement, and two abrupt drops (arrow heads) in the force are evident. (Inset) The network consisting of actin filaments (cyan) and ABPs (red) with a microbead (blue) at a bead displacement of 2 μm .

DISCUSSION

Two assays, one with a single molecule and another with a 3-dimensional network have been utilized to probe unbinding and unfolding of filamin cross-linking actin filaments. For direct comparison between single molecule and network preparations, both assays have

been prepared with similar components and performed on the same instrument platform. In the single molecule assay, one actin filament is immobilized on a rigid surface while the other filament is bound to a gelsolin-coated microsphere. By pulling the bead using an OTFS, the force is applied to a single filamin/F-actin complex and results in either unbinding of actin filaments from filamin or unfolding of filamin subdomains. In the second, network assay, a microsphere is translated through a cross-linked actin gel while monitoring the resistive force. Because the microsphere is comparable in size to the gel microstructure, discrete events (drops in force) are observed, that can be related to individual rupture or unfolding events. Comparison of these two types of measurement provides new insights into the detailed nature of actin cross-linking by filamin.

In the single molecule assays, unbinding is characterized by a clear snapback of the bead to the baseline after rupture, analogous to the abrupt force drops seen in AFM measurements. But unlike AFM, the optical trap allows us to continue pulling on the bead after the rupture event and to simultaneously observe its trajectory in the x - y plane. This additional information allows us to observe and identify both unfolding and unbinding events. Unbinding is characterized by an abrupt drop in force, followed by a different pulling trajectory when (and if) the force rises again (see, e.g., Figs. 2a and 2b), signifying that the point of attachment between the two actin filaments has moved. This could result either from the same filamin rebinding at another binding site along the same filament or a

different actin filament, or from a second filamin bound at a different site coming into play and supporting the load. Transitions that do not relax back to baseline suggest unfolding, conformational changes, or rapid rebinding to the same site or to a different one very near to the first. Evidence supporting the conclusion that the site of binding remains the same comes from the pulling trajectories; if, as the force rises again, the subsequent trajectory follows the first, the site of attachment must be at, or very near, the initial one. Our results show that $>86\%$ of the transitions where the force relaxes back to baseline exhibit a different pulling trajectory indicating multiple unbinding events. As just discussed, this can be explained by reattachment of the tethered actin filament or multiple bindings formed on the substrate-bound filaments.

Unfolding of ABP filamin is generally characterized by a regular sawtooth pattern exhibited in the force-extension curve. In these repeating transitions, the force does not relax back to zero and the pulling trajectories all lie along the same curve. The number of apparent force drops in the unfolding regime varies from 8 to 17, fewer than the 24 potential unfolding Ig domains of filamin. In cases for which the distance between force drops is irregular and larger, unfolding of several Ig domains may occur simultaneously. Also, the actin filament can unbind from filamin before all 24 subdomains of the filamin unfold. When the unbinding and unfolding events are grouped and analyzed separately, the levels of force required are found to be quite similar (70 ± 23 pN for unbinding and 57 ± 19 pN for unfolding) supporting this hypothesis. In our previous measurement at the low loading rate of 5–50 pN/s,⁹ unbinding of filamin dominated and only a couple force drops were observed in the potential unfolding traces. Therefore, the distinct multiple transitions observed in this study suggest that loading rate is a critical factor in determining the likelihood of consecutive unfolding events. To further identify the unfolding of filamin, the distances between force peaks were calculated and the average period of the repeating pattern was found to be 28 nm. Each Ig domain of filamin consists of 96 amino acids. Assuming the distance between amino acids is 3.5 Å,² the theoretical change of contour length is expected to be ~ 34 nm. Previously, Furuike *et al.* used an AFM to extend filamin directly and showed that the unfolding occurs in the force range between 50 to 220 pN, leading to ~ 30 nm change in the contour length.¹⁰ We have also observed a decrease in slope of the force-extension curves during unfolding, which is similar to the abrupt change of force slope in both AFM and OTFS measurements of unfolding.^{3,10,21,38} However, compared to the flattening of the slope observed in AFM measurements,^{3,10} the peak force we observe continues to increase during

consecutive unfolding. One important difference between our measurements with the optical trap and measurements by AFM is that the latter applies a tensional load directed from the point of surface tethering to the point of attachment to the AFM probe. In contrast, the load is applied indirectly by pulling an actin filament, and filamin in our assay experiences shear and torsional deformation as well as tension during pulling. In addition, the increase in length of filamin due to unfolding also causes a change in assay geometry resulting in a change in force application. These differences might help to explain why, in AFM extension, more Ig domains of filamin tend to unfold prior to rupture. The complex but more physiologically relevant geometry of our assay may increase the possibility of unbinding after unfolding of several domains. As a result, relatively irregular and fewer repeats of undulation are exhibited compared to the regular sawtooth-like behavior observed in the AFM measurement.¹⁰

One particularly interesting finding is that the critical forces for unbinding and unfolding are quite similar, suggesting that both are likely to be important mechanisms in regulating cytoskeletal mechanics and thereby influencing a wide range of dynamic behaviors. Two events occurring at the same force can confer a higher degree of modulation of cell responses to stress. Unfolding can allow for added compliance with the ability for the cytoskeleton to recover to its initial configuration when loads are relaxed. Unbinding, on the other hand, allows for shape remodeling of the cell. What factors regulate the tendency for one mechanism over the other remains unclear, although we have observed both at the similar force level.

A unique feature of our measurement method was that we could observe the dependence of unbinding force on the pulling angle between the two cross-linked actin filaments. This led to the observation that the rupture force significantly decreases when the pulling angle exceeds 45° . While the force at zero angle stretches the cross-linking protein, the force applied with non-zero angle causes a twisting deformation to be applied to the bond (Inset in Fig. 5a). Our results suggest that bonds rupture more easily when they are subject to a torque/shear force. Since the same angle-dependent behavior with the similar critical angle $\sim 45^\circ$ was also observed in our previous measurements at low loading rate,⁹ this implies that the molecular structure of the ABP-actin bond rather than the dynamic loading condition determines the threshold angle. Compared to filamin, the rupture force for α -actinin exhibited a lower dependence on angle except at the largest angles, $>70^\circ$. Because both filamin and α -actinin share a similar actin binding-domain, the smaller critical angle for filamin seems to be due to the

larger molecular weight and complex structure. Filamin A is a 280 kDa protein with an actin binding domain at its N-terminus followed by 24 tandem immunoglobulin-like repeats which are interrupted by two hinge regions; one between repeats 15 and 16 and the other between repeats 23 and 24.¹⁷ Dimerization through the last C-terminal repeat forms a V-shaped homodimer, which is quite different from the short and antiparallel α -actinin dimer. Tests for filamin mutants such as the hinge-less one will be useful for identifying which subdomain plays a significant role in determining a torsional rigidity.

In vivo ABPs and actin filaments are organized into a three-dimensional actin cytoskeleton. External stress or internal tensions generated by actomyosin contraction can create various types of loading conditions on cross-linking proteins, such as extension, compression, shear, and torsion; these different conditions, as the present results demonstrate, can influence the force levels for rupture or unfolding. Events associated with network fracture or nonlinear rheology have been suggested to occur at levels force smaller than the plateau value of single molecule rupture force,^{11,37} suggesting that the cross-linking bonds in the network undergo complex deformations. Numerical simulations were useful to help explain how molecular interactions influence the mechanical behavior of the network. The force on the bead exhibited an abrupt decrease when a cross-linking protein unbinds, similar to the transitions observed in the experiments. However, the force at which the force drop occurred was higher compared to the experiments for both single molecule and F-actin network.

This difference in force could be caused by discrepancies between the experiment and simulation in terms of system size, filament length, and loading speed.

Combining experiments and computational analysis suggests that unbinding could account for the abrupt transitions observed during bead translation through a cross-linked actin network. At this time, however, we can not rule out the possibility that similar transitions might occur as a result of filament buckling or unfolding of ABPs. Further analysis with additional experiments in entangled F-actin solutions will be helpful in elucidating the microscopic origin of network collapse and consequential strain-softening.

ACKNOWLEDGMENTS

Support from the NIGMS (GM076689), the NSF Career Award (0643745), the Nicholas Hobson Wheelers, Jr. Fellowship, the W. M. Keck Foundation, the Westaway Research Fund, and the Singapore-MIT

Alliance for Research and Technology are gratefully acknowledged. Filamin and gelsolin were generously supplied by F. Nakamura and T. P. Stossel. We also wish to thank W. Hwang for useful discussions.

REFERENCES

- ¹Bell, G. I. Models for specific adhesion of cells to cells. *Science* 200:618–627, 1978.
- ²Berg, J. M., J. L. Tymoczko, and L. Stryer. *Biochemistry*. New York: W. H. Freeman, p. 1100, 2002.
- ³Bhasin, N., P. Carl, S. Harper, G. Feng, H. Lu, D. W. Speicher, and D. E. Discher. Chemistry on a single protein, vascular cell adhesion molecule-1, during forced unfolding. *J. Biol. Chem.* 279:45865–45874, 2004.
- ⁴Brau, R. R., P. B. Tarsa, J. M. Ferrer, P. Lee, and M. J. Lang. Interlaced optical force-fluorescence measurements for single molecule biophysics. *Biophys. J.* 91:1069–1077, 2006.
- ⁵Bursac, P., G. Lenormand, B. Fabry, M. Oliver, D. A. Weitz, V. Viasnoff, J. P. Butler, and J. J. Fredberg. Cytoskeletal remodelling and slow dynamics in the living cell. *Nat. Mater.* 4:557–561, 2005.
- ⁶Dearruda, M. V., S. Watson, C. S. Lin, J. Leavitt, and P. Matsudaira. Fimbrin is a homolog of the cytoplasmic phosphoprotein plastin and has domains homologous with calmodulin and actin gelation proteins. *J. Cell Biol.* 111:1069–1079, 1990.
- ⁷Evans, E., and K. Ritchie. Dynamic strength of molecular adhesion bonds. *Biophys. J.* 72:1541–1555, 1997.
- ⁸Fabry, B., G. N. Maksym, J. P. Butler, M. Glogauer, D. Navajas, and J. J. Fredberg. Scaling the microrheology of living cells. *Phys. Rev. Lett.* 87:148102, 2001.
- ⁹Ferrer, J. M., H. Lee, J. Chen, B. Pelz, F. Nakamura, R. D. Kamm, and M. J. Lang. Measuring molecular rupture forces between single actin filaments and actin-binding proteins. *Proc. Natl. Acad. Sci. U.S.A.* 105:9221–9226, 2008.
- ¹⁰Furuike, S., T. Ito, and M. Yamazaki. Mechanical unfolding of single filamin A (ABP-280) molecules detected by atomic force microscopy. *FEBS Lett.* 498:72–75, 2001.
- ¹¹Gardel, M. L., F. Nakamura, J. Hartwig, J. C. Crocker, T. P. Stossel, and D. A. Weitz. Stress-dependent elasticity of composite actin networks as a model for cell behavior. *Phys. Rev. Lett.* 96:088102, 2006.
- ¹²Gardel, M. L., F. Nakamura, J. H. Hartwig, J. C. Crocker, T. P. Stossel, and D. A. Weitz. Prestressed F-actin networks cross-linked by hinged filamins replicate mechanical properties of cells. *Proc. Natl. Acad. Sci. U.S.A.* 103:1762–1767, 2006.
- ¹³Gibson, L. J., and M. F. Ashby. The mechanics of 3-dimensional cellular materials. *Proc. R. Soc. A* 382:43, 1982.
- ¹⁴Gibson, L. J., M. F. Ashby, G. S. Schajer, and C. I. Robertson. The mechanics of two-dimensional cellular materials. *Proc. R. Soc. A* 382:25–42, 1982.
- ¹⁵Gittes, F., and C. F. Schmidt. Back-focal-plane detection of force and motion in optical traps. *Biophys. J.* 74:A183, 1998.
- ¹⁶Goldmann, W. H., and G. Isenberg. Analysis of filamin and alpha-actinin binding to actin by the stopped flow method. *FEBS Lett.* 336:408–410, 1993.
- ¹⁷Gorlin, J. B., R. Yamin, S. Egan, M. Stewart, T. P. Stossel, D. J. Kwiatkowski, and J. H. Hartwig. Human endothelial

- actin-binding protein (Abp-280, nonmuscle filamin)—a molecular leaf spring. *J. Cell Biol.* 111:1089–1105, 1990.
- ¹⁸Guo, B., and W. H. Guilford. Mechanics of actomyosin bonds in different nucleotide states are tuned to muscle contraction. *Proc. Natl. Acad. Sci. U.S.A.* 103:9844–9849, 2006.
- ¹⁹Hummer, G., and A. Szabo. Kinetics from nonequilibrium single-molecule pulling experiments. *Biophys. J.* 85:5–15, 2003.
- ²⁰Ingber, D. E. Cellular tensegrity: defining new rules of biological design that govern the cytoskeleton. *J. Cell Sci.* 104(Pt 3):613–627, 1993.
- ²¹Kellermayer, M. S. Z., and C. Bustamante. Folding-unfolding transitions in single titin molecules characterized with laser tweezers. *Science* 277:1117, 1997.
- ²²Kim, T., W. Hwang, and R. D. Kamm. Computational analysis of a cross-linked actin-like network. *Exp. Mech.* 49:91–104, 2009.
- ²³Kumar, S., I. Z. Maxwell, A. Heisterkamp, T. R. Polte, T. P. Lele, M. Salanga, E. Mazur, and D. E. Ingber. Viscoelastic retraction of single living stress fibers and its impact on cell shape, cytoskeletal organization, and extracellular matrix mechanics. *Biophys. J.* 90:3762–3773, 2006.
- ²⁴Kwiatkowski, D. J., P. A. Janmey, and H. L. Yin. Identification of critical functional and regulatory domains in gelsolin. *J. Cell Biol.* 108:1717–1726, 1989.
- ²⁵Lang, M. J., C. L. Asbury, J. W. Shaevitz, and S. M. Block. An automated two-dimensional optical force clamp for single molecule studies. *Biophys. J.* 83:491–501, 2002.
- ²⁶McGough, A., M. Way, and D. DeRosier. Determination of the alpha-actinin-binding site on actin filaments by cryoelectron microscopy and image analysis. *J. Cell Biol.* 126:433–443, 1994.
- ²⁷Merkel, R., P. Nassoy, A. Leung, K. Ritchie, and E. Evans. Energy landscapes of receptor–ligand bonds explored with dynamic force spectroscopy. *Nature* 397:50–53, 1999.
- ²⁸Miyata, H., R. Yasuda, and K. Kinoshita. Strength and lifetime of the bond between actin and skeletal muscle alpha-actinin studied with an optical trapping technique. *Biochim. Biophys. Acta Gen. Subj.* 1290:83–88, 1996.
- ²⁹Nakamura, F., E. Osborn, P. A. Janmey, and T. P. Stossel. Comparison of filamin A-induced cross-linking and Arp2/3 complex-mediated branching on the mechanics of actin filaments. *J. Biol. Chem.* 277:9148–9154, 2002.
- ³⁰Neuert, G., C. Albrecht, E. Pamir, and H. E. Gaub. Dynamic force spectroscopy of the digoxigenin-antibody complex. *FEBS Lett.* 580:505–509, 2006.
- ³¹Neuman, K. C., and S. M. Block. Optical trapping. *Rev. Sci. Instrum.* 75:2787–2809, 2004.
- ³²Shin, J. H., M. L. Gardel, L. Mahadevan, P. Matsudaira, and D. A. Weitz. Relating microstructure to rheology of a bundled and cross-linked F-actin network in vitro. *Proc. Natl. Acad. Sci. U.S.A.* 101:9636–9641, 2004.
- ³³Storm, C., J. J. Pastore, F. C. MacKintosh, T. C. Lubensky, and P. A. Janmey. Nonlinear elasticity in biological gels. *Nature* 435:191–194, 2005.
- ³⁴Stossel, T. P., J. Condeelis, L. Cooley, J. H. Hartwig, A. Noegel, M. Schleicher, and S. S. Shapiro. Filamins as integrators of cell mechanics and signalling. *Nat. Rev. Mol. Cell Biol.* 2:138–145, 2001.
- ³⁵Suzuki, N., H. Miyata, S. Ishiwata, and J. K. Kinoshita. Preparation of bead-tailed actin filaments: estimation of the torque produced by the sliding force in an in vitro motility assay. *Biophys. J.* 70:401–408, 1996.
- ³⁶Tees, D. F. J., R. E. Waugh, and D. A. Hammer. A microcantilever device to assess the effect of force on the lifetime of selectin–carbohydrate bonds. *Biophys. J.* 80:668–682, 2001.
- ³⁷Tharmann, R., M. M. A. E. Claessens, and A. R. Bausch. Viscoelasticity of isotropically cross-linked actin networks. *Phys. Rev. Lett.* 98:088103, 2007.
- ³⁸Tskhovrebova, L., J. Trinick, J. A. Sleep, and R. M. Simmons. Elasticity and unfolding of single molecules of the giant muscle protein titin. *Nature* 387:308–312, 1997.
- ³⁹Wachsstock, D. H., W. H. Schwarz, and T. D. Pollard. Cross-linker dynamics determine the mechanical properties of actin gels. *Biophys. J.* 66:801–809, 1994.
- ⁴⁰Xu, J. Y., D. Wirtz, and T. D. Pollard. Dynamic cross-linking by alpha-actinin determines the mechanical properties of actin filament networks. *J. Biol. Chem.* 273:9570–9576, 1998.
- ⁴¹Yuan, C., A. Chen, P. Kolb, and V. T. Moy. Energy landscape of streptavidin–biotin complexes measured by atomic force microscopy. *Biochemistry* 39:10219–10223, 2000.